

Gamma Probe for Revealing Cancerous Cells

Anastasia Yagnyukova¹, Dmitry Mikhaylov², Timur Khabibullin³,
Andrey Grigorenko⁴ and Leonid Panfilov⁵

*National Research Nuclear University "MEPhI" (Moscow Engineering Physics Institute),
Kashirskoe highway 31, 115409, Moscow, Russian Federation*

*E-mail: ¹<yagn.anastasia@gmail.com>, ²<dmmikhajlov@mephi.ru>,
³<t_khabibullin@ecmephi.ru>, ⁴<agrigorenko.mail@ecmephi.ru>, ⁵<lapanfilov@ecmephi.ru>*

KEYWORDS Gamma Probe. Gamma Ray Detection. Cancer Detection. Lymph Node. Radiopharmaceutical

ABSTRACT This paper deals with the development of the compact wireless gamma probe for malignancies diagnostics. It defines the location of a 'guardian' lymph node (the lymph node closest to the tumor) and defines the size of the tumor, helping establish the stage of disease, the radicalism of the forthcoming operation and the subsequent treatment methods. The gamma probe detects gamma radiation from radiopharmaceuticals accumulating in places of concentration of metastasis, thus revealing cancerous lymph nodes. This paper provides a description of the gamma probe prototype. The main characteristics of the gamma probe were measured, and some problems and were discovered, along with possible solutions. Simulation of the gamma probe was run to determine the optimal configuration of the collimator. Some tests on laboratory animals were run, yielding important measurements, which proved the prototype gamma probe able to quickly and accurately locate the areas of the radiopharmaceutical's densest concentration within the body.

INTRODUCTION

Recognition of oncology diseases using radionuclide diagnostics is today the major task of nuclear medicine among the wide range of other tasks (Giammarile 2014; Brouwer 2014; Von Meyenfeldt 2014; Bogliolo 2015). Radionuclide or radioisotope diagnostics is a section of radio diagnosis designated for detecting pathological changes in human organs and tissues using radiopharmaceuticals that interfere with physiological processes in the body.

Diagnostic equipment used in radionuclide medicine generally consists of a detector, an analyzing and converting unit, and a storage device. Amongst such devices, the compact gamma locator, or gamma probe, is specifically designed to identify localized areas of accumulation of radiopharmaceuticals within the body (Wengenmair 2005; Gamma Probes 2014; Grigorenko 2015).

Gamma probes are mostly used in the detection of intraoperative sentinel lymph nodes (SLN) and non-invasive scanning of the patient to

identify superficial malignant neoplasms (Belyaev 2010; Ikram 2013; Bellotti 2013; Mihaljevic 2014; Wei 2015). In cancer staging, the SLN procedure is the most common method to assess the stage to which a cancer has progressed (Dusi 2000; Chen 2006; Da Costa 2006; Sarikaya 2008).

The first method is carried out as follows. Before the operation, the patient is given radiopharmaceuticals that accumulate in the very nidus of the tumor, and in the network of nearby lymph nodes affected by metastases. The surgeon removes the tumor and then removes the lymph nodes, which are in turn checked for metastasis with a gamma probe. Since the network of lymph nodes in the body is a diverging network, a one-by-one check for metastasis is a reliable means by which to establish the extent to which metastasis has spread throughout the body. This procedure can reduce the invasiveness of the tumor removal procedure and save the maximal amount of healthy tissue without the risk of recurrence.

The second method is completely non-invasive and is an addition to traditional radionuclide procedures. In some cases (superficial location of the tumor, its small diameter) using single-photon emission computed tomography (SPECT) or positron emission tomography (PET) imaging of the whole body is irrational, since the cost of a single procedure is important. Due to the limited number of scanners per medical

Address for correspondence:

Dmitry Mikhaylov
National Research Nuclear University "MEPhI",
Kashirskoe Highway 31, 115409,
Moscow, Russian Federation
Telephone: +7 9037548744
E-mail: polynna@yandex.ru

center, their capacity is low (Romanova 2013). In such cases, the rational option is to conduct a local radio diagnostic procedure in the area in proximity to the tumor. The procedure comprises administering radiopharmaceuticals to the patient and subsequent scanning of the location of the malignancy using a portable gamma ray detector (Karamat 2015).

Today many scientists focus their research on probes for cancer detection use. Some developments include non-invasive probes, while others focus on the creation of invasive types of probes. Both types open new opportunities for data collection, which could ease the work of surgeons and other medical specialists.

The outstanding results in targeting cancer with modern positron emitting radiopharmaceuticals have inspired the development of a number of handheld beta probes to assist in surgeries. The development and initial testing of one such probe, a miniature beta-sensitive detector unit, was developed and initially tested by Raylman and Hyder (2004). It proved suitable for use in minimally invasive procedures.

Barber et al. (2007) developed imaging devices small enough to be incorporated in medical probes and inserted into the gastrointestinal tract, imaging concentrations of tumor-seeking radiotracers.

There is another interesting piece of work on nuclear probes and their use as radiation detectors in surgery to get information about the distribution of a radioactive labeled structure. The research was conducted by Navab et al. (2008) and his team. They extended the existing nuclear probes with a spatial localization system in order to generate functional 3D surface images or functional tomographic images that can be extremely useful in the operating room.

Another example is two types of miniature gamma ray endoscopic probes developed for insertion into a body cavity to detect invisibly small or deeply located tumors. One of them is a single detector system using a small BGO ($\text{Bi}_4\text{Ge}_3\text{O}_{12}$) crystal connected with a fiber optic light guide, and the other is a dual detector system using a pair of single detector probes of the same size combined with a random coincidence technique. This research is described by Dhanasopon et al. (2005).

Existing developments show good results. However, they may have a number of disadvantages such as accuracy, size, power consumption and high cost.

This paper provides results of compact wireless gamma probe development for radio-diagnosis of carcinoma. The gamma probe detects gamma radiation from radiopharmaceuticals that accumulate in places of metastasis concentration and so reveal cancerous lymph nodes. The gamma probe will be able to define how deeply metastasis has penetrated into tissues.

METHODOLOGY

A prototype of a gamma probe for intraoperative use following interstitial injection of a radiopharmaceutical to locate regional lymph nodes by their radioactivity has been designed and developed. The prototype comprises a detecting part and the electronics. The sensitive part of the detector is made of a scintillation crystal $\text{LaBr}_3:\text{Ce}$ ($5 \times 10 \text{ mm}^3$ cylinder) and a photo detector SiPM Hamamatsu $3 \times 3 \text{ mm}^2$. Electronic components are placed on a multilayer printed circuit board mounted within the cylindrical plastic body (Fig. 1).

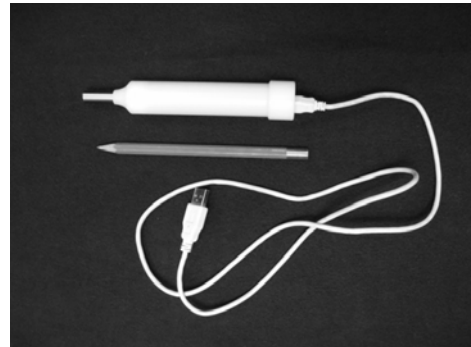


Fig. 1. Layout of gamma probe prototype
Source: Author

The voltage bias supply for the SiPM and the discrimination threshold adjustment is by way of a personal computer (PC), which is connected to the probe via a USB cable. The output (detector count rate) is displayed on the PC screen. Special software has to be installed on the PC to communicate with the gamma probe.

Details of the count rate of the detector during each measurement are stored in a text file, which allows further processing of the results.

Circuit Configuration

The electronics unit of the gamma probe consists of a voltage bias supply for the SiPM and

an amplification discrimination circuit of the analogue signal detector. The direct voltage transducer DC-DC MAX 1932 (DC is a direct current) is powered with the voltage from the computer's USB connector (+5 V). DC output is set from +25 to +75 V. Precise adjustment of the bias voltage is achieved by energizing a second SiPM voltage contact of the same polarity value from 0 to 1000 mV. The voltage is set programmatically using a digital to analogue converter (DAC).

The analogue signal from the photo detector is supplied to an amplifier and then to a comparator on which by means of DAC the desired reference voltage U_{ref} is set. At the output of the comparator information already in digital format is fed to the input of a field programmable gate array (FPGA), which is programmed to perform the necessary operations on the data from the detector.

A block diagram of a prototype gamma-probe is shown in Figure 2. The electronics module is configured as a compact printed circuit board (Fig. 3). The circuit allows for the mounting of a second SiPM and organization of the coincidence circuit.

It is notable that such a configuration of the gamma probe has a significant drawback, as a fixed connection with the PC is required, the prototype cannot be tested in the operating room,

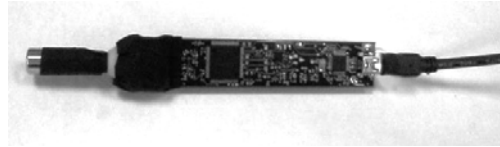


Fig. 3. Physical configuration of printed circuit board

Source: Author

and the data output to the monitor is inconvenient for doctors. Further development of the probe provides a new prototype responding to the following recommendations of radiologists and surgeons (FSBI 'Medical Radiological Research Centre', Russian Ministry of Health, Obninsk, Russia):

- ♦ Wireless data transmission
- ♦ An additional data output unit (a monitor for digital display of the detector count rate)
- ♦ Audible indication of detector count rate
- ♦ Miniaturization of the printed circuit board and the body of the probe
- ♦ Storing data on a miniature memory card for further detailed analysis

Possibility of signal output both in digital and in analogue form (for spectrometric detector characteristics studies).

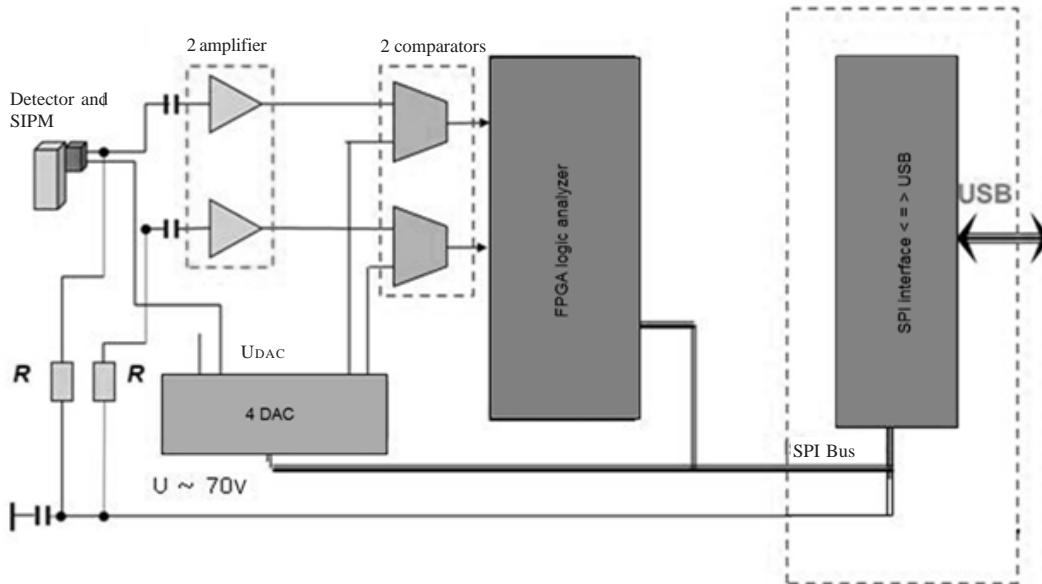


Fig. 2. A block diagram of a prototype gamma probe

Source: Author

Collimation

The protection for the sides of the sensitive part of the gamma radiation provides the cone with a narrow field of view of the detector. Moreover, reducing the diameter of the collimator's hole means improving the spatial resolution of the instrument. However, this inevitably leads to a loss of efficiency of the detector.

A tungsten cylinder with 2 mm wall thickness and inner diameter of 5 mm was produced for the prototype of the gamma probe (Fig.4).



Fig. 4. Sensitive part of the gamma probe protected with a tungsten collimator
Source: Author

Selection of the Optimal Collimator: Computer Simulation

Several computer simulations of gamma probe were conducted to determine the optimal configuration of the collimator. The Gate v6.1 framework was used for Monte Carlo simulation allowing the development of detector system models using Geant4 libraries (2014). Gate v6.1 is an advanced open source software dedicated to numerical simulations in medical imaging and radiotherapy (Gate, 2014). Three types of collimators were examined including simple cylindrical (Fig. 5), cylindrical with varying holes at the end (Fig.6), as well as a cylinder with a cone at the end (Fig. 7).

In the case of the collimator of type (1) wall thickness varied, in the case of type, and (2) the radius of the hole at the end varied. In the case of collimator of type (3) length and inner radius of the cone varied.

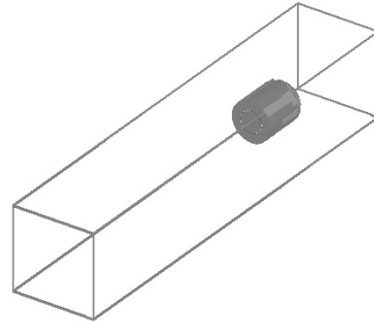


Fig. 5. Simple cylindrical collimator (1)
Source: Author

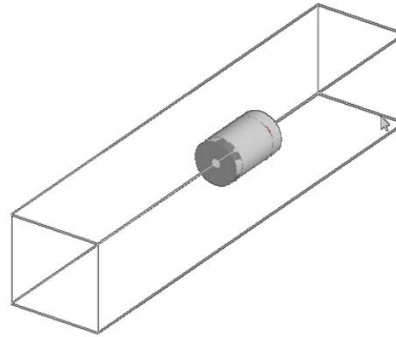


Fig. 6. Collimator with a hole at the end (2)
Source: Author

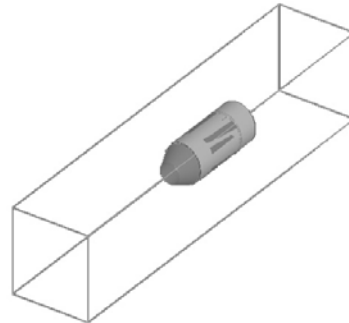


Fig. 7. Collimator with a cone at the end (3)
Source: Author

The collimator's specifications include a light grasp, spatial resolution and spatial selectivity. As spatial resolution and selectivity decline when the light grasp ratio increases, the purpose of the simulation is to choose a configuration with

an optimal compromise between all specifications of the system.

It is notable that the priority of each individual criterion depends on the type of tumor. Table 1 presents a list of some types of tumors, and a “+” denotes the significance of the probe’s parameters (Wengenmair 2005).

Consequently, the choice of the collimator should not only take into account the system’s specification, but also the future scope for the probe. It is consistent to have a set of interchangeable collimators, the most suitable for each individual case.

Description of the Model

Mathematical modeling of the gamma probe was performed using the package Gate v6.1, with subsequent processing of the data in Matlab R2010b framework (Matlab (2014) is a high-level language and interactive environment for numerical computation, visualization, and programing).

The simulation algorithm can be divided into the following stages:

1. Description of the model in the Gate framework
 - a. Setting the system’s geometry: size and relative position of components of the detector and materials.

The model describes a detector consisting of a cylindrical scintillation crystal $\text{LaBr}_3:\text{Ce}$ (radius 2.5 mm, length 10 mm), aluminum capsules with a scintillator inside (aluminum thickness 0.2 mm), and a tungsten collimator of different types.

- b. Description of the physics of interaction of gamma rays with the detector’s material.

The model describes the physical processes occurring during the interaction of low-energy gamma rays (photoelectric effect, Compton scattering, Rayleigh scattering) and electrons (the ionization energy losses, radiation losses, multiple scattering) with the matter.

- c. Source description.

The gamma-ray source in the model is a Co-57, as it was used to get the experimental data.

- d. Simulation of the electronics.

The Gate v6.1 package allows the simulation of the analogue signal processing using a Digitizer unit. The discrimination threshold is set on (100 keV), dead time for the system is introduced (~100 ns), and the energy resolution of the detector is determined (8% at 662 keV). Values are chosen based on experimental work with the detector.

- e. Definition of the format of the output data.

The Gate output data are at the same time the initial data for a Matlab program. This explains the choice of the ASCII (American Standard Code for Information Interchange) format for output information, as it is universal for both virtual environments.

- f. Setting of the required statistics/dataset time.

When modeling each experiment, the dataset time was determined so that the resulting statistics provided a fractional error of no more than a few percent.

2. Data processing in Matlab.
 - a. Reading the output Gate data.
 - b. Building the necessary distributions and graphs.
 - c. Calculation of the relevant parameters of the gamma probe.

Modeling: The Effectiveness of Gamma Rays

The efficiency of gamma rays at different distances between the detector and the source was measured in order to verify the mathematical model. The configuration of the collimator followed that of the prototype, that is, a tungsten cylinder with inner radius of 2.5 mm and wall thickness of 2 mm. A series of measurements was conducted, and the distance between the source and the detector was changed from 100 cm to 250 cm. Co-57 was selected as the simulated gamma ray source. Its activity equaled the activity of the laboratory source, which provided

Table 1: Significance of the probe’s parameters according to different types of tumors’

	<i>Melanoma</i>	<i>Breast cancer</i>	<i>Prostate cancer</i>	<i>Tumour of neck, talpa</i>
Detection efficiency	+	+	+	+
Spatial selectivity		+	+	+
Spatial resolution	+ (head, neck, collar bone)			+

ed the corresponding experimental data ($3 \cdot 10^5 \text{Bq}$).

Figure 8 shows the geometry of the model. A point source is located on a line passing through the axis of the detector. The distance between the source and the detector is measured with 10 mm steps. The dataset time for each point is 100 seconds.

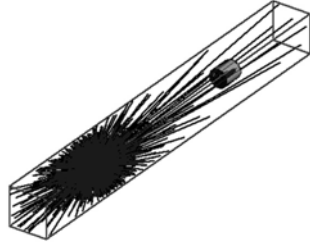


Fig. 8. Measurement geometry of detection efficiency

Source: Author

The measurement results are presented in Figure 9. The solid line in the graph is the calculated number of gamma rays emitted by the source into the solid angle of the detector per time unit. It represents one hundred percent detection efficiency. Square dots indicate the number of particles registered by the detector in the simulation, and triangular points correspond to the experimental data (see part 3 Experiments).

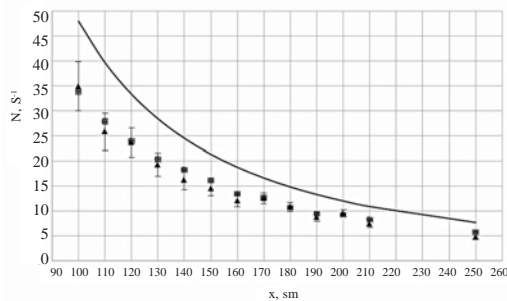


Fig. 9. Detector's counting rate - distance from the source relationship; square pixels are model, triangulars are experiment.

Source: Author

Detection efficiency of gamma rays is determined by the detector's count rate of the number of particles emitted at a given solid angle per unit/time ratio. It is constant for every value of the distance between the source and the detector. Detection efficiency was 73 ± 2 percent.

Detection efficiency depends on the scintillator material and remains constant with various configurations of the collimator. Therefore, it is consistent to determine the light grasp of the detector in order to compare the collimators.

The light grasp of the detector with a simple cylindrical collimator (1) at the distance of 100 mm is $1.05 \cdot 10^{-4}$. Since this type of collimator corresponds to the maximum fraction of particles entering the detector (in comparison with other collimators), this value is taken as one hundred percent, and the detector's light grasp with other collimators will be normalized to it.

Modeling Spatial Resolution

Spatial resolution is defined as the minimum distance between two point sources, with which they are individually distinguishable. In the case of a single point source, the measure of spatial resolution is full width at half maximum of the dependence of the detector's count rate on the location the source on the line perpendicular to the axis of the detector.

Geometry of the model is shown in Figure 10.

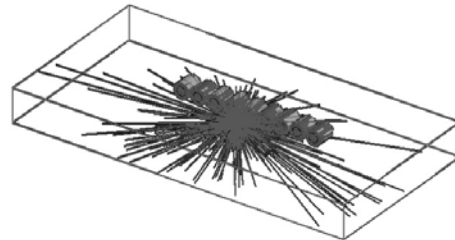


Fig. 10. Geometry of the experiment to determine the spatial resolution of the detector

Source: Author

The distance between the detector and the source is 10 mm, and the dataset time is 10 seconds. The measurement result for one of the types of collimator (type 1) is shown in Figure 11.

For convenience in defining the half-width of the histogram, this was approximated by a Gaussian distribution (Lehmann 1997). Sample statistics is $\sim 10^5$ particles in the peak, meaning that the fractional error of the spatial resolution is ~ 0.1 percent.

Simulation: Spatial Selectivity

Spatial selectivity of the gamma probe is determined by the slope angle, at which the detec-

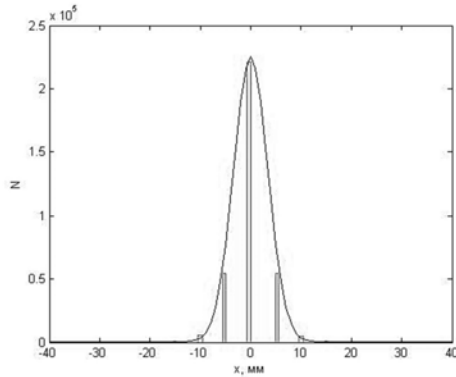


Fig. 11. Coordinate distribution of the detector's count rate
 Source: Author

tor must be rotated regarding the source, so that the count rate halved.

Measurement geometry is shown in Figure 12. Distance from the source to each detector is 30 cm, and the angle varies from -90° to 90° with a step of 16° . Dataset time was 100 seconds. The measurement result for one of the types of collimators (type 1) is shown in Figure 13.

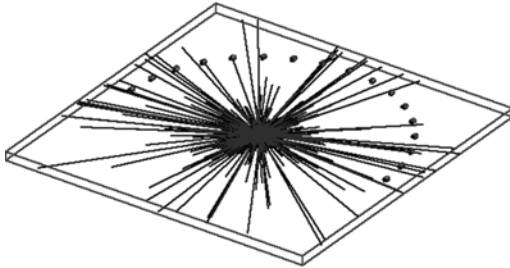


Fig. 12. Measurement geometry of the experiment to determine the spatial selectivity of the detector
 Source: Author

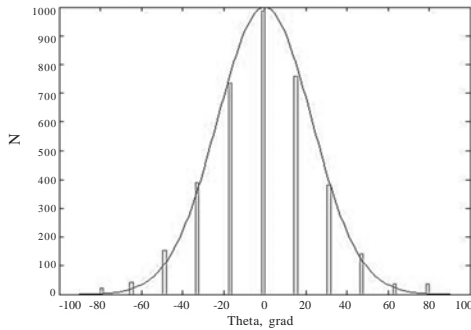


Fig. 13. Angular distribution of detector count rate
 Source: Author

The histogram is approximated by a Gaussian distribution for the convenience of calculation of the half width.

Statistics of about 10^3 particles provides a fractional measurement error of about five percent.

The Simulation Results

Measurements of light grasp, spatial resolution and spatial selectivity were taken for three types of collimators, namely, open cylinder, the cylinder with a hole in the front end and the cylinder with a conical front part. In the first case, the cylinder wall thickness varied (from limiting case, without a collimator, to a thickness of 2 mm). In the second type of the collimator the radius in the front end varied from 2.5 mm (open end) to 1 mm. In the case of a conical end of the collimator, the inner radius of the cone and its length varied.

The simulation results are shown in Table 2. The table shows that the use of tungsten collimator with a wall thickness more than 1 mm is inconsistent, but the tungsten cylinder with a thin wall is fragile and difficult to manufacture and operate.

As a conclusion, it can be noted that the optimum configuration is a cylinder with a cone at the end, since it allows the light grasp value to be kept at almost the same level as in the case of open collimator, while greatly improving the spatial resolution, and is the only collimator which it is able to improve spatial selectivity.

RESULTS




The developed prototype was tested. Measurements of the main characteristics of gamma probe, such as spatial resolution, spatial selectivity and the efficiency of detection of gamma rays were taken.

Laboratory gamma ray source of Cs-137 (662 keV) and Co-57 (80% of 122 keV and 136 keV, 10%) was used. All measurements were made using a tungsten collimator with inner radius of 2.5 mm and wall thickness of 2 mm.

Integral Spectrum of Cs-137

The prototype gamma probe is unable to output the analogue signal from the detecting part to the standard spectrometric tract, but vi-

Table 2: Simulation of a probe with different types of collimators (compared to the light-grasp of the detector with an open cylinder collimator (Type 1))

Collimator type	Wall thickness, mm	Inner radius, mm	Outer radius, mm	Length, mm	Light-grasp, %*	Spatial resolution, mm	Spatial selectivity, °
Cylinder	No collimator	2.5	-	10	100	12.5	-
	0.5		3		100	8.2	27
	1		3.5		100	7.8	25
	1.5		4		100	7.8	25
	2		4.5		100	7.8	25
Cylinder with a closed end	2	1	4.5	12	19	2.4	19
		1.5			37	4.5	19
		2			68	5.2	19
		2.5			95	6.9	19
Cylinder with a cone at the end	2	1	4.5	15	18	4.5	13
		1.5			34	5.4	13
		2			67	6.9	13
		2.5			95	7.8	13
	2	2.5	4.5	12	96	14.4	23.6
				13	96	10.6	16
				14	96	9.9	15.9
				15	96	7.8	13

sualization of the energy spectrum is very important in terms of properly selecting the discrimination limit and evaluating the general accuracy of the detector.

It is known that the integral and differential energy spectra are in a one-to-one relation, that is, the integral spectrum is a histogram of pulses from the detector, having amplitude above the threshold. Therefore, values of each point of the integral of the spectrum can be obtained by summation of the differential spectrum to the left of the threshold.

Thus, there is a special feature in the area of the photopeak in both differential spectrum and integrated spectrum. This fact was verified by means of a package of Matlab R2010b. An expected integral spectrum was graphed (Fig. 14 b) based on the previous measurements in the energy spectrum of the source of Cs-137 (Fig. 14 a). The figures clearly state that in the region of the left edge of the photopeak on the integral spectrum there is a sloping area in the differential spectrum. Thus, using a gamma probe of the integrated spectrum and setting a discrimination threshold in the middle of the sloping area allows the cutting off of events associated with Compton scattering.

Experimental data proved that a sloping area is present in the integral spectrum of the source of Cs-137 (Fig. 15, highlighted in dashed lines).

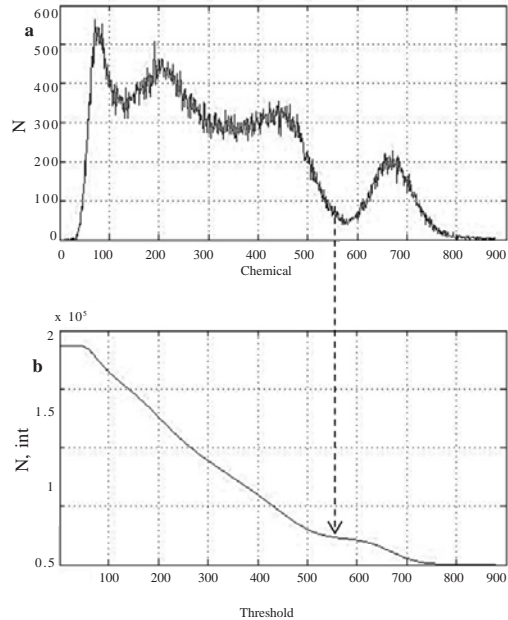


Fig. 14. a. Differential spectrum of Cs-137; b. Integral spectrum, based on differential spectrum.
Source: Author

The integral spectrum was obtained by recording the detector count rate as a function of the discrimination threshold programmatically exposed.

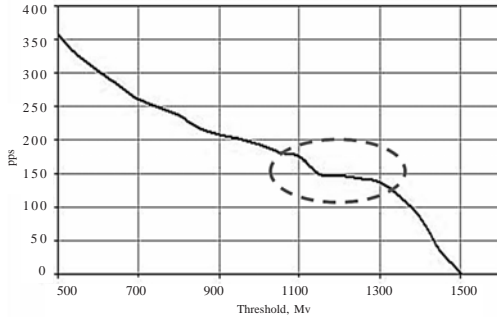


Fig. 15. The integral spectrum of the source of Cs-137 (662 keV)
 Source: Author

SiPM Temperature Instability

During the measurements a decrease in the detector count rate over time (Fig. 16) was discovered.

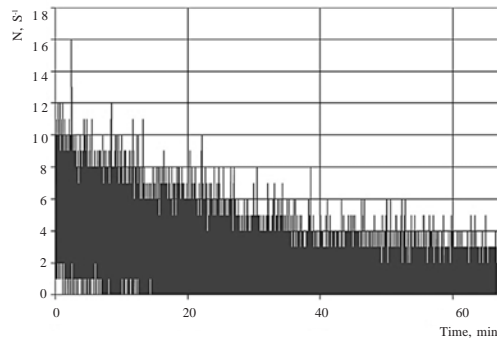


Fig. 16. Counting rate – time relationship
 Source: Author

Investigation of the problem revealed that the decrease in the count rate is due to the thermal instability of the silicon photomultiplier in operating mode the photodiode heats and SiPM gain falls with increasing temperatures, and the temperature increase necessitates a corresponding increase in the value of the operating bias voltage that must energize SiPM to keep the gain.

Special measurements were taken in a thermostat and an obtained experimental plan was graphed in order to define the nature of the relationship between the working voltage and temperature measurements. Figure 17 shows that the dependence is linear. The index is $56 \text{ mV}/^{\circ}\text{N}$.

There are two options for the temperature compensation of bias voltage, and both are

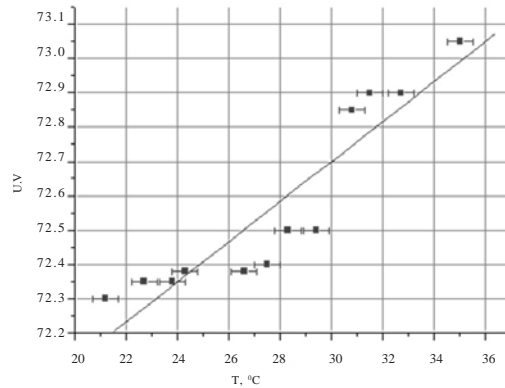


Fig. 17. Operating voltage bias – working temperature SiPM dependence
 Source: Author

based on the inclusion of a thermistor in the charge. In one of them, changing the thermistor resistance value is digitized and converted into code, which is then input to the DAC and sets the necessary additional voltage on the second SiPM contact. The second method is analogue, which is a thermistor and is included in the feedback circuit, provided by developers of the voltage converter MAX 1932.

Figure 18 (MAX1932 2007) shows a typical circuit with the NTC-thermistor (negative temperature coefficient) in a voltage conversion circuit.

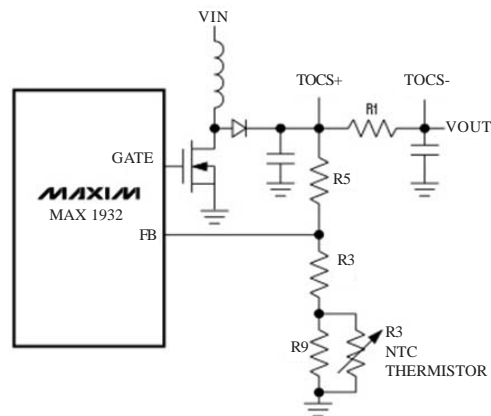


Fig. 18. Schematic diagram of the inclusion of the thermistor
 Source: Author

The analogue method of thermal stabilization was implemented. The required ratio of voltage change per degree Celsius bias is provided

by selecting the rating value for resistors R5, R8, R9 in Figure 18. First, operation of the proposed scheme was verified using a multi-turn trimmer resistor. Manual changing of its resistance simulated the thermistor. The expected linear dependence of the voltage and 'imaginary temperature' was obtained.

Further measurements were taken directly from the thermistor. The measurement result is shown in Figure 19. The graph shows the output voltage compensation of circuit MAX 1932 on the temperature, and the dependence is linear with the compensation factor of 40 mV/°C.

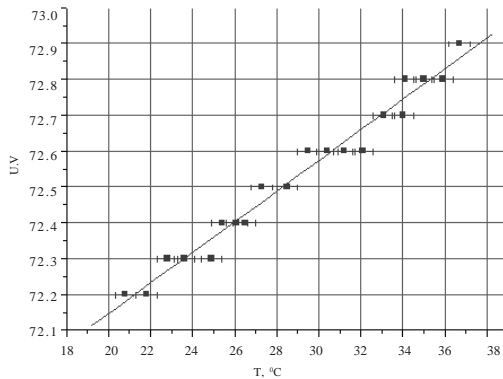


Fig. 19. Compensation of the voltage bias using a NTC-thermistor
Source: Author

Gamma Ray Detection Efficiency

Measurements of gamma ray detection efficiency were taken on a Co-57 source, as its line (124 keV) is close in energy to the line of the most common medical radioisotope Tc-99m (140 keV) and Cs-137 (662 keV). These measurements have the effectiveness of a single geometry (only one distance between source and detector), but at several points were taken in order to test the results. Efficiency value must be maintained at different distances between the source and the detector.

The measurement results for the Co-57 and Cs-137 are shown in Figure 20 (up and down respectively).

The calculated curves of the detector count rate and the distance from the source dependence, in the approximation of a point source at one hundred percent efficiency is shown in the graphs along with the experimental data. Thus,

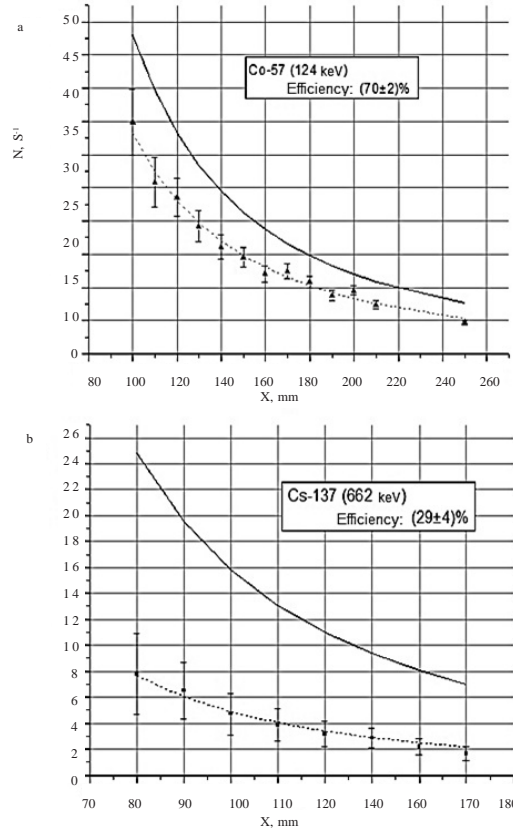


Fig. 20. The dependence of counting rate of the detector on distance from the source, a. for Co-57, b. for Cs-137
Source: Author

the efficiency of the detector is the ratio of the count rate on the experimental curve to the calculated value of the counting rate at a given distance.

The effective detection of Gamma ray was 70 ± 2 percent for Co-57 (124 keV) and 29 ± 4 percent for the Cs-137 (662 keV). These values are constant over the whole range of distances shown in the graph, for both sources.

Experimental points are well approximated by the dependence of $1/R^2$ type, and hence in the present range of the point source's distances, approximation is valid.

Sensitivity of the detector was also measured. It is determined as the number of pulses per second recorded by the detector, referred to one kBq of source activity measured at the very end of a sensitive part of the locator. This value reached 12 c/s/kBq at the Co-57 source.

Spatial Resolution and Spatial Selectivity

Spatial resolution describes the minimum distance between two point sources on which they can be registered separately. The dependency of the detector count rate for the source position along a line perpendicular to the axis of the detector should be measured in order to determine the spatial resolution (Fig. 21). Full width at half maximum of the distribution (FWHM) is the estimation of the spatial resolution.

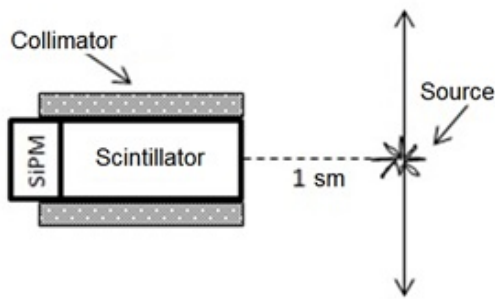


Fig. 21. Scheme for spatial resolution measuring
Source: Author

The inner diameter of the scintillator is 5 mm, and the wall thickness of the tungsten collimator is 2 mm.

Projection distance between the detector and the source of the detector onto the axis is selected to be 1 cm, since this is a typical arrangement of nodes at the depth of the human body.

Spatial selectivity is the angular resolution of the detector. Spatial selectivity is determined as detector count rate dependence on the polar angle between the detector axis and the line connecting the source and the detector (Fig. 22). FWHM of this distribution is the estimation of spatial selectivity.

The measurement results are shown in Figure 23 (spatial resolution, SR) and Figure 24 (spatial selectivity, SS). FWHM value was 8 mm and 26°, respectively. All measurements were taken with a Co-57 source (124 keV).

Laboratory Tests on Animals

The prototype gamma probe was tested on a laboratory rat, which was given “Tehnefor” (^{99m}Tc-EDTMP) radiopharmaceutical. The medication is bone-tropic and accumulates mainly in the bones of the skeleton. About forty percent

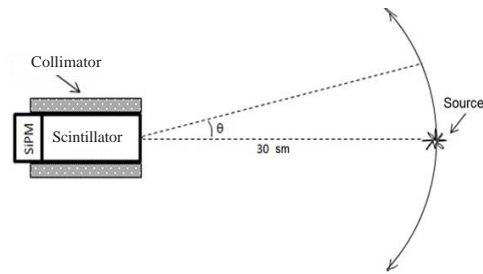


Fig. 22. Scheme for spatial selectivity measuring
Source: Author

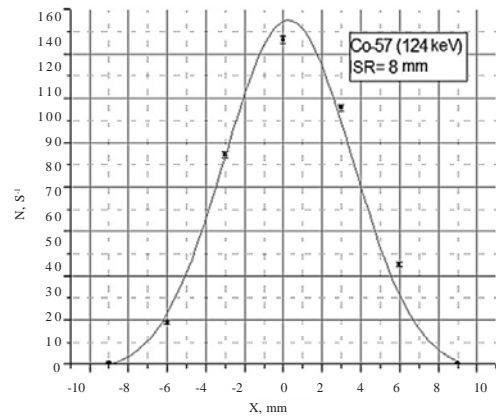


Fig. 23. Dependence of the counting rate on the transverse coordinate between the detector and the source. FWHM = 8 mm.
Source: Author

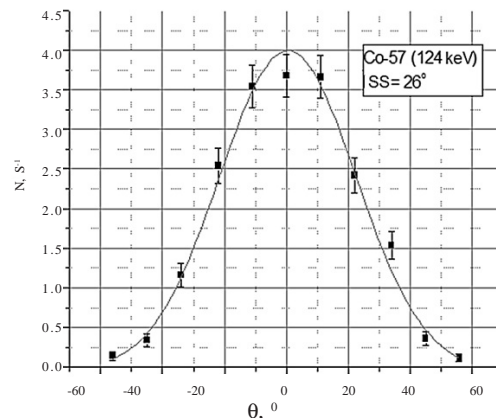


Fig. 24. Dependence of the counting rate on the polar angle between the detector and the source. FWHM = 26°
Source: Author

of the given dose is excreted by the kidneys. In the study, three hours after being administered most of the radiopharmaceutical was detected in the rat's bladder, which measures ~1 cm. This allowed the device to be tested in conditions close to its real application areas.

Figure 25 (left) shows a diagram of the rat's body scan. A net was put on the rat, and the count rate was recorded in the net's nodes. A picture shown in Figure 25 (right) was obtained based on this two-dimensional array of values using Matlab R2010b packet. The Figure shows that apart from the region of maximum accumulation of the radiopharmaceutical (bladder), other soft tissues are also visible, and the contour of the body is clearly portrayed.

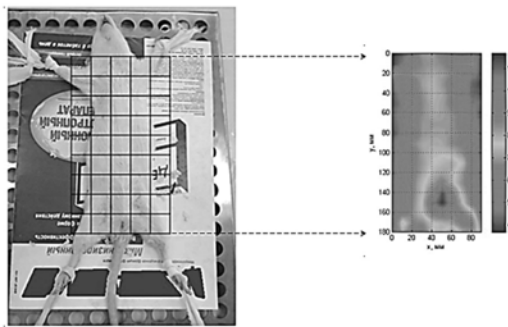


Fig. 25. Photo of the lab rat and radiopharmaceutical accumulation image obtained by gamma probe
Source: Author

Based on the same data a three-dimensional surface graph showing the difference in the count rate in the maximum accumulation area of the radiopharmaceutical (in comparison with neighboring areas) was created (Fig. 26).

CONCLUSION

The proposed prototype of the gamma probe for revealing cancerous cells in tissues was com-

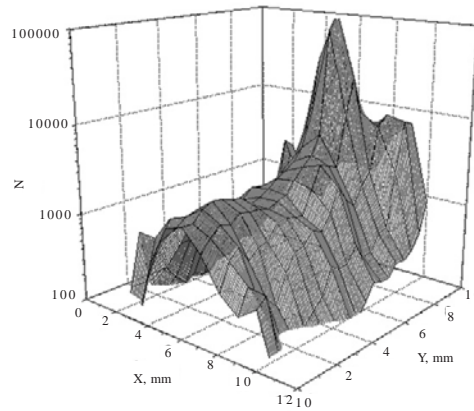


Fig. 26. Spatial distribution of the counting rate
Source: Author

pared with analogues, namely, Europrobe CsJ, Eurorad, C-Trak Omni-Probe and Neoprobe. The results of measurements of principal parameters of the gamma probe and their comparison with their Western analogies are shown in Table 3.

The prototype is no worse than foreign analogues. Its spatial resolution and selectivity are particularly notable as advantages of the gamma probe. When in operating conditions, portability and the ability to control the device with a small PC are of particular importance.

However, more studies with radiopharmaceuticals should be conducted, including preclinical tests on animals with model diseases and clinical tests on patients.

RECOMMENDATIONS

The proposed gamma probe will significantly increase the effectiveness of patient examination and allow detecting metastases in organisms. It will help prevent severe forms of oncological diseases. Portability of the device and the opportunity of control with the help of a small computer play a great role in an operating room.

Table 3: Comparison of parameters of gamma probes

Manufacturer (country)	Coordinate resolution, mm	Spatial selectivity, °	Sensitivity, imp/s/kBq
Europrobe CsJ, Eurorad (France)	14	35	7
C-Trak Omni-Probe, Care Wise (USA)	15	50	23
Neoprobe 2000 (USA)	15	36	10
Gamma-probe (Russia, NRNU MEPhI)	8	26	12

In the future, it is planned to finish the stage advanced development for the gamma probe, prepare commercial design for the device, and to organize small lot manufacturing and develop working constructing documents.

The device needs clinical testing.

REFERENCES

- Barber HB, Barrett HH, Wild WJ, Woolfenden JM 2007. Development of small in vivo imaging probes for tumour detection. *IEEE Transactions on Nuclear Science*, 31(1): 599-604.
- Bellotti C, Castagnola G, Tierno SM, Centanini F, Sparagna A, Vetrone I, Mezzetti G 2013. Radioguided surgery with combined use of gamma probe and hand-held gamma camera for treatment of papillary thyroid cancer locoregional recurrences: a preliminary study. *European Review for Medical and Pharmacological Sciences*, 17(24): 3362-3366.
- Belyaev VN, Brantova OS, Emelyanova IV 2010. Gamma-probe based on a semiconductor photodetector for rapid diagnosis of cancer. *Medical Physics*, 2: 42-47.
- Bogliolo S, Marchiole P, Sala P, Giardina E, Villa G, Fulcheri E, Menada MV 2015. Sentinel node mapping with radiotracer alone in vulvar cancer: A five year single-centre experience and literature review. *European Journal of Gynaecological Oncology*, 36(1):10-15.
- Brouwer OR, Van Den Berg NS, Mathéron HM, Van Der Poel HG, Van Rhijn BW, Bex A, Van Tinteren H, Valdés Olmos RA, Van Leeuwen FWB, Horenblas S 2014. A hybrid radioactive and fluorescent tracer for sentinel node biopsy in penile carcinoma as a potential replacement for blue dye. *European Urology*, 65(3): 600-609.
- Chen SL, Iddings DM, Scheri RP, Bilchik AJ 2006. Lymphatic mapping and sentinel node analysis: Current concepts and applications. *A Cancer Journal for Clinicians*, 56(5): 292-309.
- Da Costa FE, Relá PR, de Oliveira IB, Pereira MCC, Hamada MM 2006. Surgical gamma probe with TlBr semiconductor for identification of sentinel lymph node. *IEEE Transactions on Nuclear Science*, 53(3): 1403-1407.
- Dhanasopon AP, Levin CS, Foudray AMK, Olcott PD, Habte F 2005. Scintillation crystal design features for a miniature gamma ray camera. *IEEE Transactions on Nuclear Science*, 52(5): 1439-1446.
- Dusi W, Angelotti P, Bollini D, Mengoni D, Morom C, Ricard M 2000. Advanced gamma-probes for radioguided oncological surgery. *IEEE Nuclear Science Symposium Conference Record*, 3: 21/118-121/123.
- Friess H, Martignoni ME 2014. Transferring innovative freehand SPECT to the operating room: First experiences with sentinel lymph node biopsy in malignant melanoma. *European Journal of Surgical Oncology*, 40(1): 42-48.
- Gamma Probes 2014. IntraMedical Imaging. From <<http://www.gammaprobe.com/products/gamma-probes>> (Retrieved on 21 April 2014).
- GATE 2014. Forewords. From <<http://www.opengate-collaboration.org>> (Retrieved on 21 April 2014).
- Geant4: A Toolkit for the Simulation of the Passage of Particles Through Matter. 2014. Last updated: 21 Mar 2014. From <<http://geant4.web.cern.ch/geant4>> (Retrieved on 1 April 2014).
- Giammarile F, Bozkurt MF, Cibula D, Pahisa J, Oyen WJ, Paredes P, Olmos RV, Sicart SV 2014. The EANM clinical and technical guidelines for lymphoscintigraphy and sentinel node localization in gynaecological cancers. *European Journal of Nuclear Medicine and Molecular Imaging*, 1-15.
- Grigorenko Andrey, Panfilov Leonid, Smirnov Alexander, Starikovskiy Andrey, Rubin Dmitry, Shulga Ekaterina, Sychev Nikolay, Nikolaeva Alexandra 2015. The existing gamma-probes review for searching functional increase and complex improvement possibilities. *Biosciences Biotechnology Research Asia*, 12(Spl. Edn. 2): 197-200.
- Ikram M, Akhtar S, Maseeh-uz-Zaman Junaid M, Dhari T, Ahmad Z, Hussain R 2013. Sentinel node localisation using pre-operative lymphoscintigraphy and intraoperative gamma probe in early oral cavity cancer. *Journal of the Pakistan Medical Association*, 63(8): 976-979.
- Karamat MI, Farncombe TH 2015. Simultaneous ^{99m}Tc and ¹¹¹In SPECT reconstruction using accelerated convolution-based forced detection Monte Carlo. *Nuclear Science, IEEE Transactions on*, 62(5): 2085-2095.
- Lehmann K 1997. Gaussian Distributions. Princeton University. From <<http://www.edasolutions.com/old/MathCad/Statistics/images/GaussianDistribution.pdf>> (Retrieved on 1 April 2014).
- MATLAB® 2014. The MathWorks, Inc. From <<http://www.mathworks.com/products/matlab>> (Retrieved on 14 April 2014)
- MAX1932 2007. Digitally Controlled, 0.5% Accurate, Safest APD Bias Supply. Maxim Integrated. Page Last Modified: 2007-07-13. From <<http://www.maximintegrated.com/datasheet/index.mvp/id/3484>> (Retrieved on 11 February 2015).
- Mihaljevic AL, Rieger A, Belloni B, Hein R, Okur A, Scheidhauer K, Schuster T, Sarikaya I, Sarikaya A, Reba RC 2008. Gamma probes and their use in tumour detection in colorectal cancer. *International Seminars in Surgical Oncology*, 5: 25.
- Navab N, Traub J, Buck AK, Ziegler SI, Wendler T 2008. Navigated Nuclear Probes for Intra-operative functional imaging. *Proceedings of 5th IEEE International Symposium on Biomedical Imaging (ISBI 2008)*, Paris, France, 14-17 May 2008, pp. 1395-1398.
- Romanova S 2013. Nuclear medicine: Status and prospects. *Remedium*, 6: 8-20.
- Raylman RR, Hyder 2004. A dual surface barrier detector unit for beta-sensitive endoscopic probes. *IEEE Transactions on Nuclear Science*, 51(1): 117-122.
- Von Meyenfeldt EM, Siebenga J, Van Der Pol HAG, Schreurs WMJ, Hulsewe KWE 2014. Radionuclide-guided biopsy of bone lesions in cancer patients: A reliable, well-tolerated technique. *European Journal of Surgical Oncology*, 40(2): 193-196.
- Wei L, Chen F, Zhang X, Li D, Yao Z, Deng L, Xiao G 2015. ^{99m}Tc-dextran lymphoscintigraphy can detect sentinel lymph node in breast cancer patients. *Experimental and Therapeutic Medicine*, 9(1): 112-116.

Wengenmair H, Kopp J 2005. Gamma Probes for Sentinel Lymph Node Localization: Quality Criteria, Minimal Requirements and Quality of Commercially Available Systems. From <[\[augsburg.de/index.php/fuseaction/download/lrn_file/gammaprobes.pdf\]\(http://www.klinikum-augsburg.de/index.php/fuseaction/download/lrn_file/gammaprobes.pdf\)> \(Retrieved on 5 February 2015\).](http://www.klinikum-</p></div><div data-bbox=)

Paper received for publication on June 2014
Paper accepted for publication on November 2015.